Instabilities in the deformation of magnetoelastic membranes

Prashant Saxena

Glasgow Computational Engineering Centre, School of Engineering
University of Glasgow, Rankine Building, Oakfield Avenue, Glasgow G12 8LT
Email: prashant.saxena@glasgow.ac.uk

Summary

We study the inflation of weakly magnetizable isotropic membranes in the presence of externally applied magnetic field. The relevant governing equations, boundary conditions, and stability criteria are derived from a variational formulation and computational solutions are obtained for three geometries – circular, cylindrical, and toroidal membranes. It is observed that magnetic field can alter the onset of elastic limit point instability and introduce new magnetic limit points. Multiple stable equilibrium configurations are predicted for a given coupled load. We also observe induction of wrinkling in the membrane due to the magnetic field.
Key Words: *magnetoelasticity; membrane; instability; limit point; wrinkling*

1 Introduction

Magnetoelastic polymers are artificially fabricated composites that can change their mechanical attributes (shape/ stiffness etc.) upon the application of an external magnetic field. Nonlinear magnetoelastic membranes have applications in inflatable systems for energy harvesting and vibration absorption. We aim to develop a computational formulation to study the deformation of magnetoelastic membranes under coupled pressure and magnetic loading while focussing on development of instabilities in the system under these extreme deformation conditions.

2 Mathematical formulation

2.1 Kinematics

Figure 1 shows three cases of incompressible isotropic nonlinear magnetoelastic membranes. The membranes are inflated by a gas pressure as well as deformed by the externally applied magnetic field as shown in the figure. The right Cauchy–Green deformation tensor $\mathbf{C}$ for each of the three cases of deformed toroidal, cylindrical, and circular membranes can be written, respectively, as

$$\begin{bmatrix} \frac{\rho^2+\eta^2}{R_s^2} & 0 & 0 \\ 0 & \frac{\rho^2}{[R_b+R_s\cos\theta]^2} & 0 \\ 0 & 0 & \lambda_3^2 \end{bmatrix}, \begin{bmatrix} u'^2+[1+w']^2 & 0 & 0 \\ 0 & \frac{[R_0+u]^2}{R_0^2} & 0 \\ 0 & 0 & \lambda_3^2 \end{bmatrix}, \begin{bmatrix} \rho'^2+\eta'^2 & 0 & 0 \\ 0 & \frac{\rho^2}{R^2} & 0 \\ 0 & 0 & \lambda_3^2 \end{bmatrix}. \tag{1}$$

We refer the reader to the papers [2, 3, 4] for detailed derivations of above expressions. Here λ_3 is the stretch ratio in the thickness direction of the membrane, ρ and η are the parameters defining the profile for the toroidal and circular membrane upon deformation while u and w are the parameters defining the profile of cylindrical membrane upon deformation as shown in figure 1.

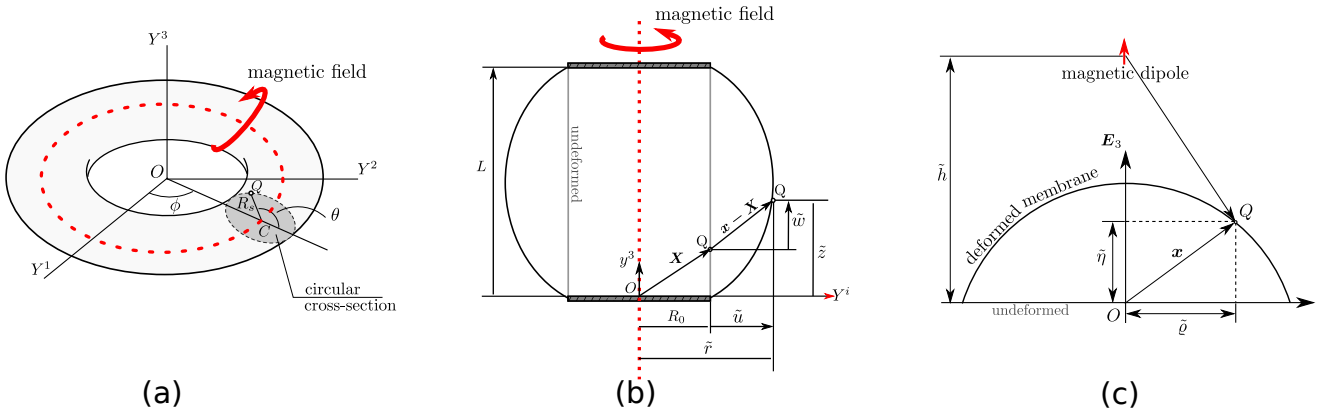

Figure 1: The three geometries studied in this work (a) Inflated toroidal membrane with magnetic field applied by a current carrying loop [2]. (b) Inflated cylindrical membrane with magnetic field applied by an infinite current carrying wire [3]. (c) Inflated circular membrane with magnetic field applied by a fixed dipole [4].

2.2 Governing equations and computational procedure

Under the thinness approximation, the total potential energy functional (E) of the system under consideration can be written as (see [1])

$$E = t_0 \int_{\Omega} \varrho\psi \, dA - t_0\mu_0 \int_{\Omega} \mathbf{m} \cdot \mathbf{h}_a \, dA - \int_{V_0}^{V_0+\Delta V} P \, dV, \tag{2}$$

where $\varrho\psi(\mathbf{F}, \boldsymbol{\mu})$ is the free energy per unit volume, $\mathbf{F}$ is the deformation gradient, $\boldsymbol{\mu}$ is the material magnetization per unit mass, $\mathbf{m} = \varrho\boldsymbol{\mu}$ is the magnetization per unit current volume, $\mathbf{h}_a$ is the externally applied magnetic field, P is the gas pressure used to inflate the membrane, Ω denotes the mid-surface of the undeformed membrane, t_0 is the initial thickness of the membrane, V_0 is the enclosed initial volume, and ΔV is the change in this enclosed volume. We use the following relations for a weakly magnetized membrane (self-generated magnetic field is negligible)

$$\frac{\partial\psi}{\partial\boldsymbol{\mu}} = \mu_0\mathbf{h}_a, \quad \varrho\psi = W + \frac{\mu_0\varrho^2}{2\chi}|\boldsymbol{\mu}|^2, \quad \mathbf{m} = \chi\mathbf{h}_a, \tag{3}$$

to simplify the above energy functional and then take the first variation to arrive at the relevant governing equations and boundary conditions for each of the three cases. Governing equations for the toroidal and circular membrane problems can be rewritten as ODEs in matrix form as

$$\mathbf{A}\mathbf{X}' = \mathbf{E}, \tag{4}$$

where $\mathbf{X}$ is an $n \times 1$ column vector of the functions to be evaluated, $\mathbf{A}$ is an $n \times n$ and $\mathbf{E}$ is an $n \times 1$ matrix both of which depend on the material parameters, loading conditions and the state variable $\mathbf{X}$. We solve the above set of boundary value problem by converting it into an initial value problem using the shooting method and coupling it with an optimization routine.

Governing equations for the cylindrical membrane problem occur in the form of coupled ODEs that are more amenable to be solved using a finite difference method coupled with a cubic extrapolation arc-length technique.

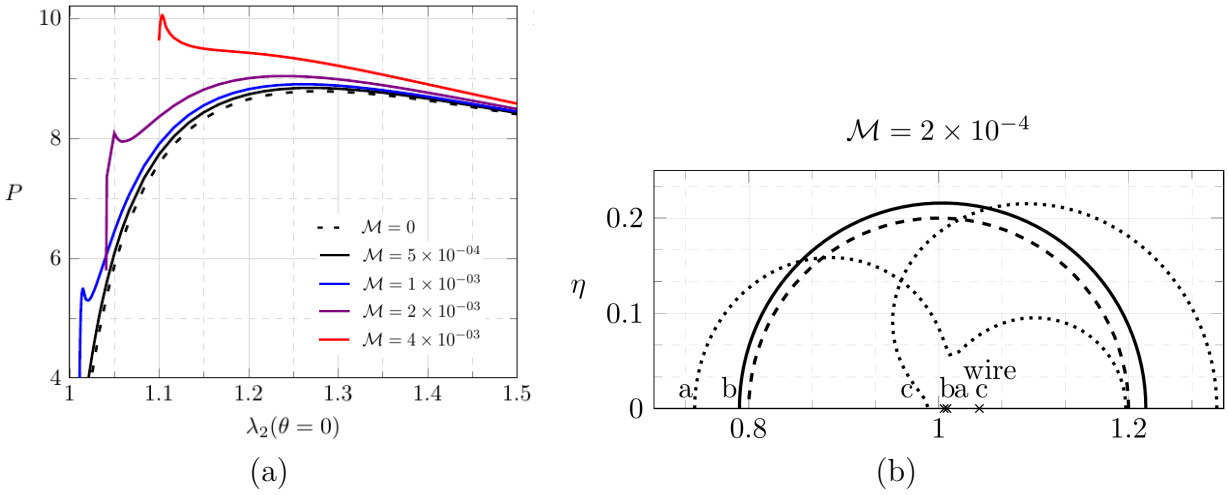

Figure 2: Results for toroidal membrane taken from [2]. (a) Pressure vs stretch plot shows change of limit point instability as magnetic loading $\mathcal{M}$ is increased. (b) Multiple stable and unstable profiles of torus cross-section for a given magnetoelastic loading.

2.3 Stability of equilibrium

A necessary condition for the equilibrium state obtained in Section 2.2 is that it be a minimiser of the functional in equation (2). Corresponding to the two matrices $\mathbf{P}$ and $\mathbf{Q}$ given below

$$\mathbf{P} = \frac{1}{2}\begin{bmatrix} \mathcal{F}_{\rho'\rho'} & \mathcal{F}_{\rho'\eta'} \\ \mathcal{F}_{\eta'\rho'} & \mathcal{F}_{\eta'\eta'} \end{bmatrix}, \qquad \mathbf{Q} = \frac{1}{2}\begin{bmatrix} \mathcal{F}_{\varrho\varrho} & \mathcal{F}_{\varrho\eta} \\ \mathcal{F}_{\eta\varrho} & \mathcal{F}_{\eta\eta} \end{bmatrix} - \frac{1}{2}\frac{d}{dr}\begin{bmatrix} \mathcal{F}_{\varrho\varrho'} & \mathcal{F}_{\varrho\eta'} \\ \mathcal{F}_{\eta\varrho'} & \mathcal{F}_{\eta\eta'} \end{bmatrix}, \tag{5}$$

the necessary condition for stability is that $\mathbf{P}$ is positive definite while a sufficient condition requires that there is no conjugate point in the domain $r \in (0, 1)$. Here $\mathcal{F}$ is the integrand of the functional in equation (2) and for the circular membrane problem it is given as

$$\mathcal{F} = W\, t_0 R_0^2 r \; - \frac{\chi}{2}\mu_0 |\mathbf{h}_a|^2 t_0 R_0^2 r \; + \frac{1}{3} P R_0^3 \left[\varrho^2 \eta' - \varrho\varrho'\eta\right]. \tag{6}$$

Stability of all the solutions obtained for equations from Section 2.2 is checked via the above criteria. Expression for the total magnetoelastic (Cauchy) stress tensor is given by

$$\boldsymbol{\sigma} = \rho\psi_{,\mathbf{F}}\mathbf{F}^T + \mu_0\left[\mathbf{h}\otimes\mathbf{h} - \frac{1}{2}[\mathbf{h}\cdot\mathbf{h}]\boldsymbol{i}\right] + \mu_0\mathbf{h}\otimes\mathbf{m} - q\boldsymbol{i}, \tag{7}$$

where q is a Lagrange multiplier due to the constraint of incompressibility. Wrinkling instability is said to occur in a membrane as soon as zero or negative stresses are encountered. We record and demonstrate the location of wrinkles but are unable to update the solution due to lack of availability of a tension field theory [5] of magnetoelasticity.

3 Results and conclusion

For the toroidal membrane, we observe from figure 2(a) that magnetic field changes the location of limit point and additionally introduces an additional very early limit point. For very large magnetic field of $\mathcal{M} = 4 \times 10^{-3}$ the downward sloping curve indicates occurrence of magnetic limit point

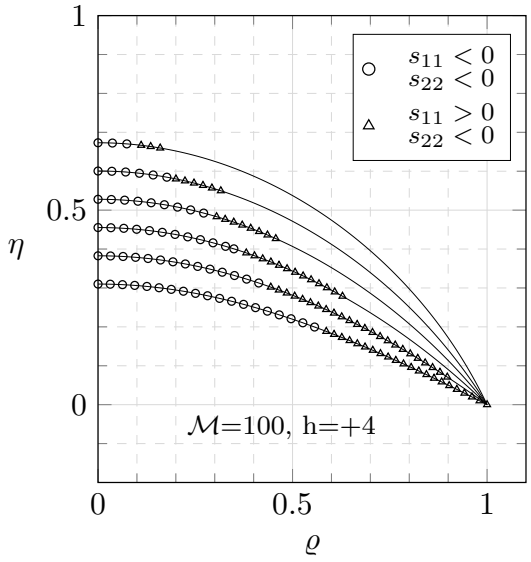

Figure 3: Profiles for circular membrane demonstrating regions of wrinkle development. Circles convey double wrinkling while triangles convey wrinkles in a single direction [4].

instability. Multiple stable and unstable equilibria for a given magnetoelastic load are shown in figure 2(b). Solid curve shows stable, dotted curve shows unstable while dashed curve represents the case where necessary condition is satisfied from section 2.3 but sufficient condition is violated. Wrinkling instability is demonstrated for circular membrane in Figure 3. We observe transition from a taut membrane (solid curve) to single wrinkles (triangles) to double wrinkles (circles) as one moves from edge of the membrane towards the centre.

Our results clearly demonstrate that magnetic loading can influence the location of limit points as well as induce additional limit point in the membrane. Occurrence of multiple stable and unstable equilibria for a given loading condition is an interesting result and needs to be studied further. We also show that compressive magnetoelastic stresses can induce wrinkles in both single and double directions in the otherwise taut membrane. We have only presented representative results here and a much more exhaustive analysis and discussion is given in references [2, 3, 4].

References

[1] M. Barham, D. J. Steigmann, M. McElfresh, R. E. Rudd, *Limit-point instability of a magnetoelastic membrane in a stationary magnetic field*, Smart Materials and Structures, 17 (2008), p. 055003.

[2] N. H. Reddy and P. Saxena, *Limit points in the free inflation of a magnetoelastic toroidal membrane*, International Journal of Non-Linear Mechanics, 95 (2017), pp. 248–263.

[3] N. H. Reddy and P. Saxena, *Instabilities in the axisymmetric magnetoelastic deformation of a cylindrical membrane*, International Journal of Solids and Structures, 136-137 (2018), pp. 203–219.

[4] P. Saxena, N. H. Reddy, S. P. Pradhan, *Magnetoelastic deformation of a circular membrane: wrinkling and limit point instabilities*, under review, (2019).

[5] D. J. Steigmann, *Tension-Field Theory*, Proceedings of the Royal Society A: Mathematical, Physical and Engineering Sciences, 429 (1990), pp. 141–173.